Photochemical & Photobiological Sciences

Accepted Manuscript

This is an *Accepted Manuscript*, which has been through the Royal Society of Chemistry peer review process and has been accepted for publication.

Accepted Manuscripts are published online shortly after acceptance, before technical editing, formatting and proof reading. Using this free service, authors can make their results available to the community, in citable form, before we publish the edited article. We will replace this *Accepted Manuscript* with the edited and formatted *Advance Article* as soon as it is available.

You can find more information about *Accepted Manuscripts* in the Information for Authors.

Please note that technical editing may introduce minor changes to the text and/or graphics, which may alter content. The journal's standard Terms & Conditions and the Ethical guidelines still apply. In no event shall the Royal Society of Chemistry be held responsible for any errors or omissions in this *Accepted Manuscript* or any consequences arising from the use of any information it contains.

ROYAL SOCIETY OF CHEMISTRY

www.rsc.org/pps

Red-emitting protein-coated conjugated polymer nanoparticles.

R. Peters,[a] L. Sandiford,[a,b] D. M. Owen,[a] E. Kemal,[a,c] S. Bourke,[a] L. A. Dailey,[c] M. Green.[a]*

a) Department of Physics,
King's College London,
Strand,
London WC2R 2LS, UK.
* mark.a.green@kcl.ac.uk

b) Department of Imaging Chemistry and Biology,
Division of Imaging Science and Biomedical Engineering,
King's College London,
4th floor, Lambeth Wing, St Thomas' Hospital,
London SE1 7EH, UK.

c) Institute of Pharmaceutical Science,
King's College London,
5th Floor, Franklin-Wilkins Building,
150 Stamford Street,
London SE1 9NH, UK.

Red emitting materials are desirable in biology due to the transparency of certain biological tissues at these wavelengths. Here, we report the synthesis of aqueous dispersions of amphiphilic protein (hydrophobin) capped red-emitting cyano-substituted poly(p-phenylenevinylene) conjugated polymer nanoparticles (CPNs) and their use in labeling live mammalian (HeLa) cells.

Conjugated polymers are a class of materials that have been widely studied, initially motivated by the excellent optical properties of such materials.[1-3] In contrast to the extensive studies of conjugated polymers in bulk and thin films,[4-6] conjugated polymer nanoparticles (CPNs) are at present a relatively new development and offer distinct advantages as potential nanometric fluorescent labels over their traditional quantum dot (QD) counterparts, due to their reduced cytotoxicity, high photostability and brightness, facile synthesis and bio-compatibility [7,8]. Furthermore, multi-functional surface modification of CPNs enables *in vitro* and *in vivo* bioimaging with specificity according to the targeting surface-bound element.

In order to successfully fulfil biological applications, it is essential that conjugated polymers disperse in aqueous solutions. One method involves modifying the polymeric side chains with charged moieties, increasing the solubility.[7] Whilst such water-soluble conjugated polymers proved successful in drug delivery and fluorescence imaging,[9-10] the availability of such materials is limited relative to the organically-soluble analogues. With this in mind, CPNs synonymous with simple preparation and purification have been proposed as an improvement. Ideally, whilst a range of emission wavelengths is desirable to allow a plurality of imaging functions, the majority of biological imaging applications favour the red end of the electromagnetic spectrum due to the transparency of certain biological tissues at these wavelengths. Whilst conjugated polymer particles have many positive attributes as biological imaging agents, few effective red emitters have been reported. Inspired by recent reports by the Chiu group of orange-emitting CPNs based on cyano-polymers,[11] we report the use of a related commerically-available material, poly(2,5-di(hexyloxy)cyanoterephtalylidene), which has emission further towards the red end of the visible spectrum when prepared as nanoparticles. The polymer, in a standard organic solvent such as THF, had an emission maximum at *ca.* 570 nm. By preparing the polymer in nanoparticulate form however, the emission was significantly redshifted to *ca*. 640 nm.

The solvatochromism of conjugated polymers is well-documented; the solubility of a given conjugated polymer in a particular organic solvent is dependent upon the atomic structure of both the solvent and solute and is directly related to the physical conformation of the solvated polymer. Consequently, solvents can be classified as either good or poor for a specific conjugated polymer based upon the favoured nanoscale conformation.[12] Conjugated polymer chains in a good solvent are proposed to adopt an extended, uncoiled conformation due to the energetically favourable interactions between the solvent molecules and polymer side chains.[13] Conversely, when placed in a poor solvent, polymer chains possess a collapsed conformation in order to minimise the energetically unfavourable solvent-solute interactions.[13] CPNs are proposed to possess a coiled polymer conformation and in this way, the spherical nanoparticulates - corresponding to the lowest free energy surface per unit volume - exist in a thermodynamically stable state, [8] regardless of the rigidity of the polymer chain. This morphology, suggesting an increase in chain folds and entanglements, can be inferred by the change in the optoelectrical properties of the nanoparticulates with respect to their behaviour in organic solvent, since the spectroscopic signatures of solvated polymers are heavily influenced by nanoscale chain organisation and chain interactions. For example, emission spectra of CN-PPV derivatives dissolved in a poor solvent reportedly presented a pronounced red-shift, with respect to that of a good solvent solution.[13,14] This may be attributed to the increased chain interactions that have a high affinity for enhanced energy transfer events as the delocalisation of the π-electrons increases.[8] This inferred that as the conjugation length increased upon CPN formation, intermolecular interactions promoted aggregation and thus presented bathochromic shifts in the emission spectra. This phenomenon was exploited to engineer a red-emitting cyano-based polymer nanoparticle system.

A further prerequisite for biomedical applications of CPNs is surface modification and functionalization. The physiochemical nature of CPNs can be effectively modified by capping the hydrophobic polymeric core with a surfactant shell.[7] Introducing a capping agent enables surface functionalization of the polymer particle, thus leading to improved biocompatibility and the potential for targeted- controlled delivery. In addition, all CPNs are inherently unstable, thus without some form of encapsulation they tend to agglomerate or coalesce rapidly.[8,15] In this way, the addition of capping agents to the CPN system is essential to provide surface passivation, improved colloidal stability and enhancement of the surface state, a fundamental parameter that influences the optoelectrical properties of CPNs.[8] It has also been reported that the fluorescent efficiency of nanoparticles may be improved by the use of capping agents,

presumably since the coated nanoparticles are able to passivate surface defects.[16] In this paper, we report the use of hydrophobins, small (~100 amino acids) amphiphilic, cysteine-rich proteins as capping agents, where the hydrophobic conjugated polymer interdigitates with the hydrophobic patch of the protein, leaving the hydrophilic, cysteine-rich structure pendant to solution inducing water solubility.

Dependent upon the hydropathy pattern of their peptide sequence and biophysical attributes, hydrophobins can be classified into two groups: Class I and Class II.[17] The increased β-sheet structure of Class I hydrophobins with respect the soluble state is suggested to account for their high stability. Conversely, membranes formed with Class II hydrophobins present significantly less stable structures, which are easily disassociated with organic solvents due to the lack of fibrillar rodlet morphology in the self-assembled monolayer.[17] To this end, Class II hydrophobins appear to be less attractive for surface modification, [18] such that only commercially-available class I hydrophobin (H* protein B, HPB) was considered as a viable CPN capping agent for emulsion stabilisation. The use of a protein as a capping agent also has the added advantage of providing amino acid groups for further potential conjugation to allow targeted delivery.

The HPB-capped CPNs were synthesised by a nanoprecipitation method. CN-PPV was dissolved in tetrahydrofuran (THF), added to an aqueous solution of the HPB and then sheared at 35 kW in an ultrasound bath. Particle dispersions were obtained after solvent evaporation and purified by centrifugation. The normalised absorption and photoluminescence spectra of the solvated polymer and concomitant uncapped and HPB-capped nanoparticulates were measured and are shown in Figure 1.

The absorption profile of the CPNs only differed slightly from that of the precursor polymer solution (Figure 1A); the aqueous nanoparticle dispersion exhibited a wider absorption profile with a flattened maximum at 457 ± 0.5 nm, with respect to that of the solvated polymer. This suggested that the extent of conjugation length heterogeneities, due to polymer chain confinement, was enhanced in HPB-capped nanoparticle assemblies. Conversely, a significant bathochromic spectral shift (72 ± 0.7 nm) was observed in the emission spectrum of CN-PPV particles with respect to that of the precursor polymer solution, (Figure 1A) pushing the emission into the red region of the visible spectrum. We take full advantage of the redshift in emission, from 569 ±0.5 nm in the parent polymer solution, to 641 ± 0.5 nm in the aqueous

particle solution to obtain a true red emitter. We suggest that this was a direct result of the change in nanoscale chain organisation and morphology upon rapid change in solvent quality. The evolution of the photoluminescence intensity of the HPB-capped CPNs as a function of time was measured, to investigate possible degradation. Over a 21-day period, the photoluminescent signal remained stable, dropping to a maximum of 80% of its initial (t=0) intensity, (Figure 1B). The emission quantum yield (QY) of the uncapped and protein-capped particles were both found to be 28 %, when excited at 480nm using an integrating sphere employing the photoluminescence method.

When the conjugated polymers assembled into nanoparticulate form, this process was accompanied by an increase in chain interactions that have a high affinity for enhanced energy transfer processes, as the delocalisation of the π-electrons increased. Upon CPN formation, unfavourable solvent-solute interactions promoted twisting of the polymer backbone, which in turn increased the spacing between adjacent atomic energy levels. The increase in polymer fold and entanglements was followed by a change in polymer conjugation length, which serves as an explanation of the observed bathochromic shift in the CPN emission spectra.

Furthermore, a slight broadening of the emission spectra for CPNs with respect to their precursor solutions was also observed. This may be attributed to the broad size distribution of the formed nanospheres. For example, it has been reported that for CPNs prepared by a self-assembly synthesis, the emission spectra were sharper since this energy-minimization procedure favoured a narrow size distribution [8]. The full-width at half-maximum (FWHM) values for the solvated polymer and CPNs, 88 ± 0.5 nm and 110 ± 0.5 nm respectively, were both relatively broad, attributable to vibronic coupling in the chromophore, the extent of which was most pronounced in the nanoparticulate form. For fluorescence-based techniques, the resulting large Stokes shift is a desirable attribute, as this corresponds to a minimal overlap of absorption and emission profiles, which in turn limits self-absorption.

An average particle core size of 35 ± 7 nm and 78 ± 16 nm was obtained for the uncapped and capped particles respectively as measured by TEM, (Figure 2A, 2B). The polymer nanoparticles were spherical, in agreement with prior work. [19,8,7] TEM size distribution histograms are presented with overlaid standard deviation. For both the uncapped and capped particle dispersions, the mean and modal particle diameter agree to within 12% error. An average hydrodynamic diameter of 110 + 35 nm and 147 ± 50 nm was obtained for the

uncapped and capped CPNs respectively, by nanosight tracking analysis (NTA), (Figure 2E, 2F). Size distributions demonstrate FWHM of *ca.* 70 nm and 100 nm for the uncapped and protein-capped CPNs respectively. The CN-PPV particle and protein-capped dispersions have a relative standard deviation (RSD) of 32% and 34% respectively indicating that the capping shell did not greatly influence the polydispersity of the nanoparticluate solutions. Both particle assemblies present a moderate width distribution. The hydrodynamic diameter of the CPNs calculated by NTA was significantly larger than the size estimated by TEM due to the protein surfactant, the hydration shell and electric dipole layer of the surrounding solvent.

To obtain a crosslinked protein shell, the amine functional groups at the N-terminus of each amino acid sequence in the side chains of lysine residues were reacted with glutaraldehyde. The hydrophobin coating was proposed to decrease surface hydrophobicity and suppress aggregation, thus leading to improved colloidal stability, a prerequisite for most biological applications. To investigate their potential use in biological imaging, laser scanning confocal microscopy was used to visualize whether the crosslinked hydrophobin-coated CPNs were internalized by HeLa cells. Z-stack images were collected with 25 slices covering a sample depth of ~12 μm, indicating that CPNs were localised inside live HeLa cells, (Figure 3), ~1hr post incubation. This cell line (human cervical carcinoma) was specifically chosen due to its association with nanodiagnostics. Orthogonal projections were reconstructed from z-scan images, confirming that the crosslinked nanoparticles were restricted to within cell boundaries, rather than extracellular components. Intracellular uptake of colloidally stable polymer nanoparticles, without the use of transfection agents, is attractive due to its simplicity and reproducibility.

In conclusion, protein-capped conjugated polymer nanoparticles have been prepared that are useful in cellular imaging. The synthesis was simple and reproducible, and the resultant CPNs presented strong emission in the red region (*ca.* 640 nm) of the electromagnetic spectrum. As a result of this exploratory cellular experiment, it is proposed that HPB polymer labels are attractive contenders towards non-toxic, photostable, fluorescent probes. We acknowledge Dr. Wendel Wohlleben and Dr. Thomas Subkowski (Material Physics Research, BASF) for supplying the proteins and for useful disucssions.

Experimental

Preperation of CN-PPV nanoparticles

All chemicals were obtained from Sigma-Aldrich, UK and used as received. Poly(2,5-di(hexyloxy)cyanoterephthalylidene) (CN-PPV) (3 mg) was dissolved in 0.96 mL THF to make a 3.125 mg/mL polymer solution. The solution was sonicated in a 35 kHz ultrasound bath at 7-9 °C, in 30 second bursts. In a separate flask, 250 µL of a hydrophobin H star protein® B stock solution (50 mg/mL) was added to 5 mL deionised water, sonicated at ambient temperature (*ca.* 20 °C) for 15 minutes, and then left for approximately 1 hour at room temperature. Then, 160 µL of the polymer solution was added to the aqueous HBP solution in a sealed flask. The mixture was sonicated at 7-9 °C in three 60 second bursts. The mixture was then left stirring in an unsealed flask for ~24 h at 400 rpm to allow solvent evaporation. The nanosuspension (~100 µg/mL CN-PPV) was subsequently filtered through filter paper and a 0.2 µm cellulose acetate syringe filter. The filtrate was washed with deionised H_2O via centrifugation at 4000 rpm for 2 minutes, a total of 5 times.

Chemical crosslinking of HPB

HPB-coated CPNs (125 µL) was diluted in 1 mL 10 mM sodium phosphate buffer (pH 7.0-7.2) and centrifuged in a 100 kDa Vivaspin® tube at 3000 rpm for 1 minute, for a total of 3 times. 500 µL of particle solution was added to 10 µL glutaraldehyde (50 wt. % in H_2O), and stirred in a sealed vial at 450 rpm for 1 hour. A disposable PD-10 desalting column was equilibrated with 50 mL of previously prepared buffer solution. The resultant crosslinked particle solution was passed through the column and 0.5 mL fractions were collected.

CN-PPV association with HeLa cells

HeLa cells were cultured as adherent monolayers in Dulbecco's Modified Eagle Medium (DMEM) supplemented with 10% heat inactivated fetal calf serum (FCS), on a sterilised 8 square well microplate. Cell cultures were kept at physiological temperature ~37◦, 5% CO2 in a humidified incubator. 250 µL of the crosslinked CN-PPV nanoparticle suspension was added to 100 µL of the aforementioned media and incubated for 1 hour. The cells were washed with phosphate-buffered saline (pH 7.0) six times. All images were acquired on a Nikon A1R+ confocal using a ×20 air-immersion objective lens of numerical aperture 0.75, with 488 nm excitation. Emission from the CN-PPV nanoparticles was collected in two channels, 570 - 620 nm and 663 - 738 nm with 2x line averaging. The brightest emission was observed in the 570 - 620 nm channel. Z-stack images were collected every 0.5 µm, with 12.5 µm sample depth. Orthogonal projections were reconstructed using Imaris software. All images are displayed with 0.2% saturation pixel thresholding.

Nanoparticle Tracking Analysis

The NanoSight® LM10 instrument employed a laser source (60 mW at 488 nm) to illuminate nanoparticles in suspension. CN-PPV CPN suspension (100 μL) was diluted in 5 mL deionised H_20 and 300 μL was injected into the flow chamber of the NanoSight® unit. The C11440-5B scientific camera was set to ×20 capture magnification with 250 camera gain. NTA 2.3 analysis software was used to generate 3 × 30 second scripts, which provided the average and modal hydrodynamic diameter, standard deviation and total concentration of the CPN suspension.

Transmission electron microscopy

TEM images were obtained using a FEI Tecnai T20 instrument with a LaB6 filament electron source operating at 200 kV accelerating voltage. The system was equipped with a FEI supertwin objective lens capable of atomic resolution and a gatan image filter, GIF 2000, which enabled energy filtration of images. Image analysis was perfomed in ImageJ software.

Quantum Yield measurements

All absolute quantum efficiency measurements were obtained using a C9920-02G Hammatsu system employing the photoluminescence method. An integrating sphere system with nitrogen gas flow was used and the entire spectral range recorded simultaneously. All samples were excited at 480 nm with a bandwidth of 5-7 nm.

Optical measurements

Absorption spectroscopy measurements were taken using a Hitachi U-4100 UV-Visible-NIR spectrophotometer in a 1 cm path length quartz cuvette. Emission spectra were obtained using a Perkin Elmer LS 50B spectrometer. Quantum yields were measured using an integrating sphere by Hamamatsu Photonics. Ltd., UK.

References

[1] S. Gunes, H. Neugebauer, and N. S. Sariciftci. *Chem. Rev.,* 107: 1324–1338, 2007.

[2] A. Mishra, C. Ma, and P. Baüerle. *Chem. Rev.,* 109: 1141–1276, 2009.

[3] G. Yu, J. Gao, J. C. Hummelen, F. Wudl, and A. J. Heeger. *Science,* 270: 1789–1791, 1995.

[4] A. J. Heeger. *Angew. Chem. Int. Ed.,* 40: 2591–2611, 2001.

[5] A. C. Grimsdale, K. Leok Chan, R. E. Martin, P. G. Jokisz, and A. B. Holmes. *Chem. Rev.,* 109: 897–1091, 2009.

[6] S. W. Thomas, G. D. Joly, and T. M. Swager. *Chem. Rev.,* 107: 1339–1386, 2007.

[7] L. Feng, C. Zhu, H. Yuan, L. Liu, F. Lv, and S. Wang. *Chem. Soc. Rev.,* 42: 620–6633, 2013.

[8] J. Pecher and S. Mecking. *Chem. Rev.,* 110: 6260–6279, 2010.

[9] D. T. McQuade, A. E. Pullen, and T. M. Swager. *Chem. Rev.,* 100: 2537–2574, 2000.

[10] K. Li and B. Liu. *Polym. Chem.,* 1: 252–259, 2010.

[11] F. Ye, C. Wu, Y. Jin, M. Wang, Y.-H. Chan, J. Yu, W. Sun, S. Hayden, D. T. Chiu, *Chem. Commun*., 2012, 48, 1778.

[12] L. Magnani, G. Rumbles, I. D. W. Samuel, K. Murray, S. C. Moratti, A. B. Holmes, and R. H. Friend. *Synth. Met.,* 84: 899–900, 1997.

[13] B. J. Schwartz. *Annu. Rev. Phys. Chem.,* 54: 141–172, 2003.

[14] I. D. W. Samuel, G. Rumbles, C. J. Collison, S. C. Moratti, and A. B. Holmes. *Chem. Phys.,* 227: 75–82, 1998.

[15] P. Wang, C. J. Collison, and L. J. Rothberg. *J. Photochem. Photobiol., A.,* 144: 63–68, 2001.

[16] T. Gutul, E. Rusu, N. Condur, V. Ursaki, E. Goncearenco, and P. Vlazan. *Beilstein J. Nanotechnol.,* 5: 402–406, 2014.

[17] K. Scholtmeijer, M. I. Janssen, M. B. M. van Leeuwen, T. G. van Kooten, H. Hektor, and H. A. B. Wosten. *Biomed. Mater. Eng.,* 14: 447–454, 2004.

[18] H. K. Valo, P. H. Laaksonen, L. J. Peltonen, M. B. Linder, J. T. Hirvonen, and T. J. Laaksonen. *ACS Nano,* 4: 1750–1758, 2010.

[19] C. Wu, Y. Zheng, C. Szymanski, and J. McNeill. *J. Phys. Chem. C.,* 112:1772–1781,2008.

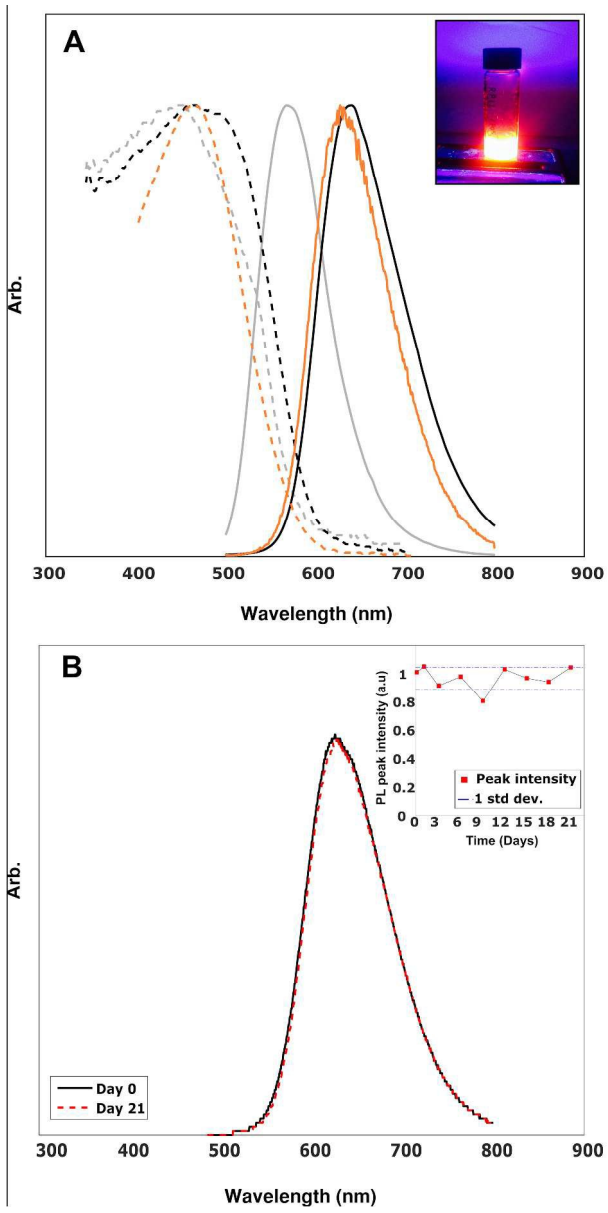

Figure 1: A) Normalised absorption (dotted lines) and emission (solid lines) spectra of CN-PPV dissolved in THF (grey lines), CN-PPV particles (orange lines) and HPB-capped CN-PPV particles (black lines). The inset shows an aqueous dispersion of hydrophobin-capped particles in ambient conditions and under 365 nm UV excitation. B) PL spectra of HPB-capped CN-PPV CPNs (λem = 640 nm) at t=0 (solid line) and t=21 days (dashed line). The inset shows the normalised emission peak intensity of the HPB-capped aqueous disperions measured over a 21 day period, and standard deviation of the mean (blue dashed lines). All samples were excited at 470 nm.

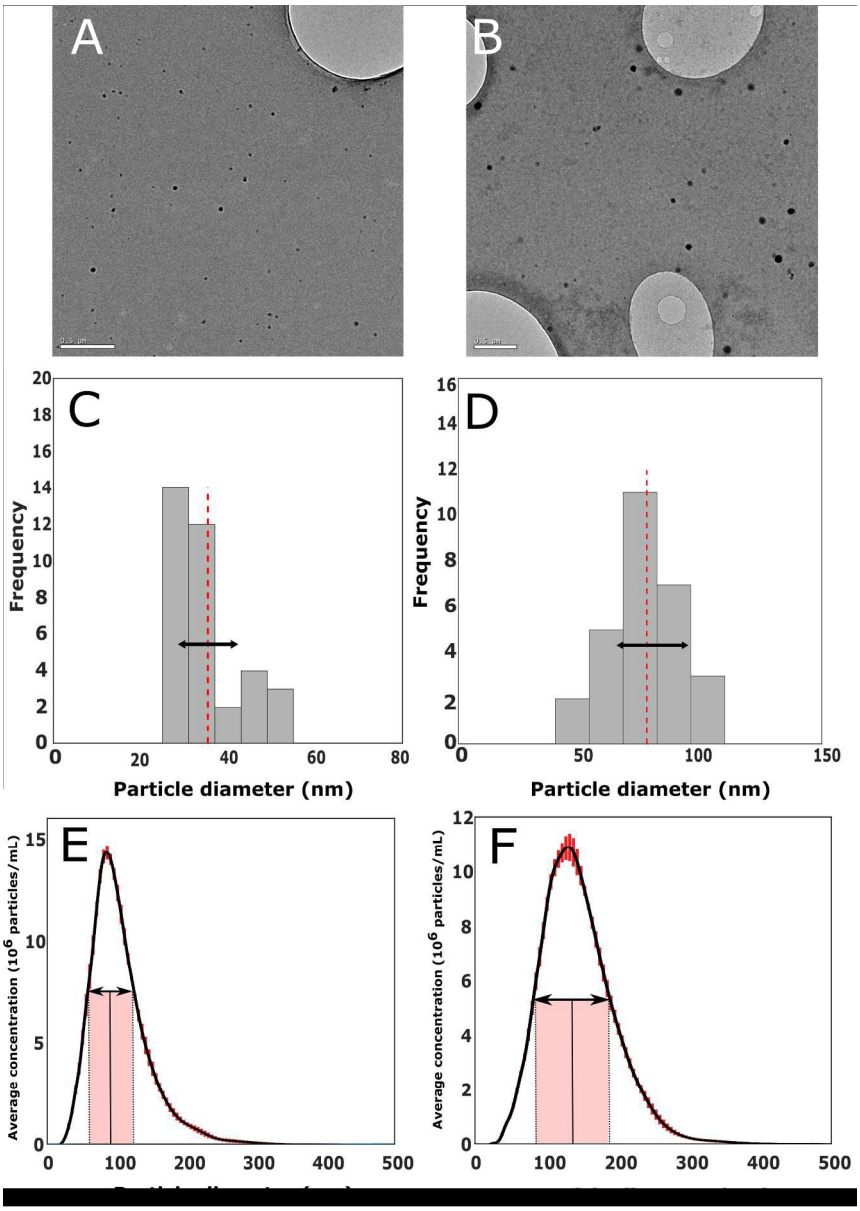

Figure 2: A-D) Representative TEM images (scale = 0.5 μm) and particle size distributions of uncapped A, C) and HPB-capped B, D) CN-PPV particles. The mean core diameters (dotted red line) and standard deviation (solid black arrows) are shown. E) Distribution curve of the hydrodynamic diameters of uncapped and F) HPB-capped CN-PPV nanoparticles with standard error of the mean (red error bars). The FWHM (solid black arrow) of the uncapped and capped CN-PPV particles are ca. 70 nm and 100 nm respectively. Both assemblies demonstrate a moderate width distribution, with 32% and 34% relative standard deviation respectively.

135x191mm (600 x 600 DPI)

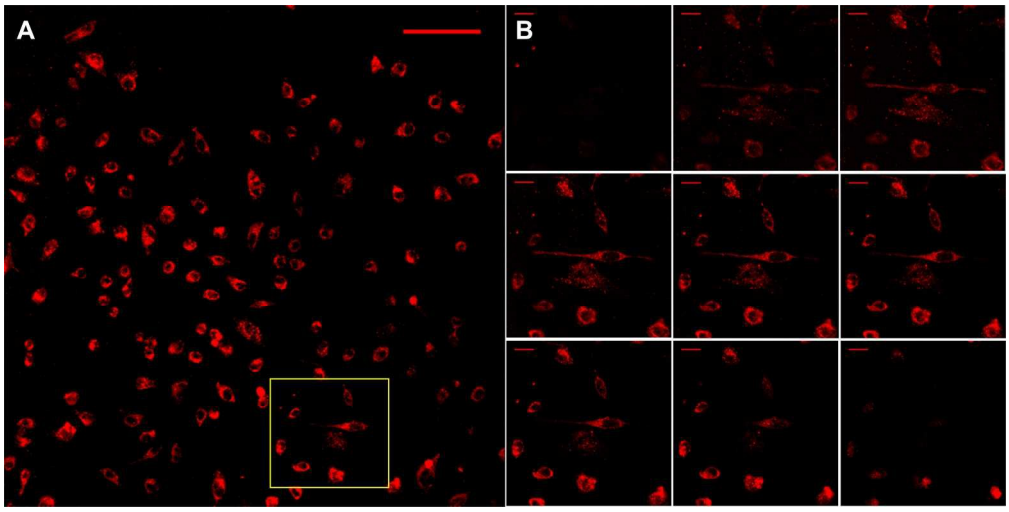

Figure 3: A) The association of crosslinked HPB-capped CN-PPV particles with cultured HeLa cells; Fluorescence was detected in the 570 - 620 nm channel with 0.2% saturation pixel thresholding. Scale bar = 100 µm. B) Z-stack through a region of interest (highlighted yellow) from the bottom of the cells to the top (left to right) at 0.5 µm steps, indicating that HPB-capped nanoparticles were internalised by HeLa cells post 1hr incubation. Scale bar = 25 µm.

224x112mm (300 x 300 DPI)

Graphical Abstract